Penerbit Akademia Baru

Journal of Advanced Research in Fluid Mechanics and Thermal Sciences

Journal homepage: www.akademiabaru.com/arfmts.html
ISSN: 2289-7879

Aerodynamic Noise Measurement In Anechoic Wind Tunnel of Rod-Airfoil With Leading Edge Serrations

Open Access

Siti Ruhliah Lizarose Samion[1], Mohamed Sukri Mat Ali[2,*]

[1] Malaysia-Japan International of Institute of Technology, Universiti Teknologi Malaysia, 54 100 Kuala Lumpur, Malaysia
[2] Department of Mechanical Precision Engineering, Malaysia-Japan International Institute of Technology (MJIIT), Universiti Teknologi Malaysia, 54100 Kuala Lumpur, Malaysia

ARTICLE INFO

Article history:
Received 23 February 2018
Received in revised form 19 May 2018
Accepted 10 June 2018
Available online 23 July 2018

Keywords:
Airfoil noise, Leading edge noise, Leading edge serrations

ABSTRACT

Turbulent flow interaction with the leading edge of an airfoil generates a well-known leading edge noise. The present work is an experimental investigation of reducing the leading edge noise by adapting serrations on the leading edge of NACA0012 airfoil. A rod is placed upstream of the airfoil to magnify the turbulence flow-leading edge interaction. Locations and the size of the serrations are two parameters being investigated for the noise reduction. The study found that a noise reduction up to 3.5 dB is obtained when the size of the serration is wider. Additionally, more sound reduction can be obtained when the angle of attack is increased.

1. Introduction

Airfoil geometry is a common part in many engineering applications, but it is also responsible for the generation of what we call as airfoil self-noise. In a strong perturbed flow, the airfoil-turbulence interaction noise (ATIN) is prominent [1-3]. The important devices involving such noise are the rotor configurations of turbo engines, helicopter rotors, and wind turbines in which the downstream airfoil blades lie in the wake of upstream blades.

The airfoil experiences fluctuating lift as a result of the unsteady pressure field produced by the airfoil in response to the turbulence. The pressure fluctuations are generated by the interaction between the turbulent eddies and the solid surface of the airfoil. Thus, part of the noise generated by this interaction is radiated to the far field and is referred to as the leading edge noise or the ATIN in this study. ATIN is mostly noticeable in the low frequency version. This is because the noise generation mechanism is dominated by the large turbulent structures.

In most experimental investigation, the upstream turbulence is generated and conveyed downstream to the airfoil by a vortex generator to create the turbulent-leading edge interaction as in the real condition. The turbulence-generating-grid is also a common mechanism by researchers to

* *Corresponding author.*
E-mail address: sukri.kl@utm.my (Mohamed Sukri Mat Ali)

have the turbulence with a full spectrum of wave number. Jackson *et al.,* [4] experimentally investigated the lift on both a two-dimensional wing and a finite aspect ratio wing subjected to grid turbulence in a closed return, low-speed wind tunnel. Turbulence was generated by a square grid of rectangular bars with 25.4 mm wide vertical bars and 6.35 mm wide horizontal bars. Paterson and Amiet [1] implemented homogeneous, isotropic turbulence field in their experiment in an open-jet, open-circuit wind tunnel with two scales anechoic chambers. The turbulence was generated using a grid with 2.54 cm bars perpendicular to the free-stream and 1.91 cm bars parallel to the free-stream. The grid has a mesh size of 13.3 cm and solidity of 0.35 and was located 11.7 mesh lengths upstream of the airfoil which allowed the turbulence to become isotropic before reaching the airfoil. Their turbulence scale was approximately 15% of the airfoil chord and had 4% turbulence intensity. They obtained that the noise associated with the interaction of the turbulence and the airfoil was an order of magnitude higher than other noise sources as the peak in the unsteady pressure was located close to the leading edge. Other several experimental investigations, like McKeough and Graham [5], Mish *et al.,* [6], Oerleman and Migliore [2], Moreau *et al.,* [3], Narayanan *et al.,* [7] and Chaitanya *et al.,* [8,9] also used grid generated turbulence in their airfoil leading edge noise experiments. However, the experimental studies of the interaction of grid-generated turbulence have created somewhat a confusing picture of the effects of the turbulence interaction with the unsteady surface. For instance, the measurement of Oerleman and Migliore [2] showed up to 5 dB increased in the noise sound level as the AOA was increased from 0° to 8° for a variety of airfoils while the experimental results of Moreau *et al.,* [3] showed almost no AOA effects on the radiated noise. This can explain the discrepancies of the far field noise measurements and the challenges to understand the interaction of turbulence with the noise generated at the leading edge. More recent experimental studies using the leading edge (LE) serrations as the ATIN reduction treatments, like Chaitanya *et al.,* [8,9] they correlated the measured turbulence spectrum with that of Von Karman's for longitudinal isotropic turbulence by Pope [10] and confirmed the turbulence generated in the isotropic is in a good degree. They presented performance of the LE serrations on the ATIN reduction and showed somewhat good correlation of the serrations geometry on the reduction mechanism with the turbulence length scale Λ, from their experiment.

Gruber *et al.,* [11] used tandem airfoil configurations in an experiment to decompose the interaction noise due to the turbulent wake of upstream airfoil and investigate its reduction due to the presence of leading edge serrations on the downstream airfoil. This study for the first time combined two airfoils to imitate a rotor-stator broadband interaction in a turbofan aircraft engine. The reductions of ATIN level has been obtained to be up to 6 dB.

In a numerical study, few types of synthetic eddy method have been implemented for inflow turbulence generation. One of them is the vortical disturbance. Turner and Kim [12] modelled a single spanwise vortex filament as the vertical disturbance. Through this approach, the resulting sound spectra are smooth making essential trends much easier to identify. Also, it is divergence free if compared to other approaches that are based on a single inflow disturbance that contain a range of frequencies. Turner and Kim [12] have made it easier explained on the discrepencies between the peak and the root of LE serrations.

Therefore, the turbulence physics upstream of airfoil is an important feature in the ATIN study as it plays the main role in the generating mechanism. Thus, it is much appreciated if any investigation of ATIN reduction can correlate the upstream turbulent characters with the reduction mechanism. The LES generally is the most promising Computational Fluid Dynamic (CFD) method to correctly predict the flows. However, extensions of the LES techniques to the prediction of ATIN generated by high Reynolds number flows in complex geometries have first to be benchmarked on relevant test cases. Such a test case must be based on geometry that contains some of the aerodynamic

mechanisms encountered in ATIN applications but remain simple enough from the computational point of view in order to achieve parametric study purposes. The rod-airfoil configuration is a relevant benchmark case for the ATIN investigation. Jacob *et al.,* [13] was among the pioneer to introduce this rod-airfoil configuration. This is because at high Reynolds numbers, the rod sheds the well-known von Karman vortex street which acts as an oncoming turbulence disturbance onto the airfoil.

The rod flows had been extensively studied since the early work of Strouhal [14] on Aeolian tones, and a complete review of this topic has been published by Zdravkovich [15]. However, although the von Karman street can be regarded as a gust, very few investigations concerning rod-airfoil configuration are reported in the literature. Stapountzis *et al.,* [16] and Cambanis [17] focused on airfoil in the near wake of a very large rod (rod diameter ≈ airfoil chord length) in the context of wind turbine. Jacob *et al.,* [14] highlighted three strong dimensional effects responsible for spectral broadening around the rod vortex shedding frequency in the subcritical regime and identified that the airfoil leading edge was the main contributor to the noise emission in a rod-airfoil configuration due to vortex-structure interaction. Takagi *et al.,* [18] investigated the influence of the cylinder transverse location on the turbulent development of the flow around the airfoil. They found that the transverse location of the cylinder impacted on the radiated acoustic field. To identify the flow features responsible for the noise generation, Henning *et al.,* [19,20] performed dual PIV and simultaneous far-field microphone measurements. Based on their correlation technique, the regularities in the near field fluctuations are related to the radiated sound. Further comparison done by Lorenzoni *et al.,* [21] revealed the ability of rod-airfoil configuration to predict reasonably well compared with the real case, especially the magnitude of the tonal peak of emission and the narrow band spectrum around it. Microphone array measurements have also been done to investigate the influences of the rod diameter and the streamwise gap between the rod and the airfoil leading edge on the broadband noise generation frequencies higher than the vortex shedding frequency [22]. The results showed that the noise generation for the lower frequencies depended more strongly on the cylinder diameter than on the streamwise gap.

Moreover, further understanding on the details of the rod-airfoil interactions have been gained through numerical simulations too [23-28]. Berland [28] found good agreement between calculation and experiment when they used direct noise calculation based on the compressible LES. The dominant noise source on the rod-airfoil model was found to be caused by impingement of Karman vortices upon leading edge of airfoil. Hence, modification of the leading edge (LE) aerodynamics can be expected to modify both the turbulent flow and the sound emission of the rod-airfoil configuration. One of the treatments implemented on the LE of airfoil is the introduction of the LE serrations. The LE serrations are inspired biologically from the silent flight of the barn owl. Many studies have proved the noise reduction promoted by LE serrations [30-34].

The use of microphone array can accurately localize noise source and determine the dominant noise at different configurations, whereas the PIV technique reveals the corresponding flow physics of the noise generation, but the use of numerical studies can also give a good flow physics behaviour based on the LES. Hence, the experimental results of current study aim to provide early expectation of using LE serrations in the NACA0012 ATIN reduction treatment before further numerical investigations can be done by the author. Current study takes the rod-airfoil configuration as the experiment case study and implemented LE serrations on the LE to investigate the noise performance. The experimental procedure is described in Section 2 and Section 3. The noise results are presented in Section 4. Finally, the conclusion from the study is given in the last section.

2. Experimental Facilities and Setup

The experiments were conducted using the anechoic open-return wind tunnel (AWT) at the University of New South Wales. The schematic diagram of the experimental setup is shown in Figure 1. The facility contains a three-dimensional contraction which goes from 1.07 m × 1.07 m to 0.455 m × 0.455 m. The contraction area ratio is 5:5:1 with turbulence intensity of $Tu = 0.6\%$. The section for mounting the test case is surrounded with a chamber with walls line with foam blocks which provide an anechoic environment.

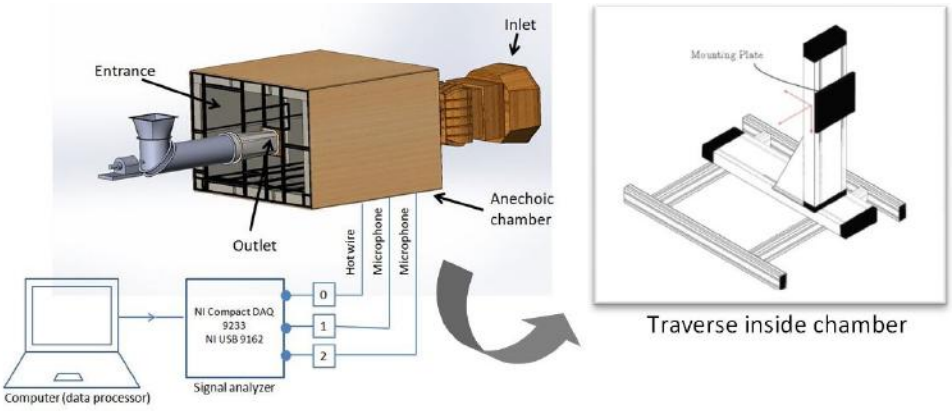

Fig. 1. Schematic diagram of experimental setup

2.1 Rod-Airfoil Configuration Setup

The rod and airfoil have a span of 455 mm and are mounted in such a manner that the ends were fixed at the mounting plates as shown in Figure 2. In this study, the coordinate system origin is located in the centre of the outlet as shown in pink lines in the sketched figure. Axis x is aligned with the streamwise direction of the flow, axis y is the cross-stream direction, and pointing to the wind tunnel wall is z the spanwise direction. For current experiment, the free stream velocity of the jet is set at 15 m/s.

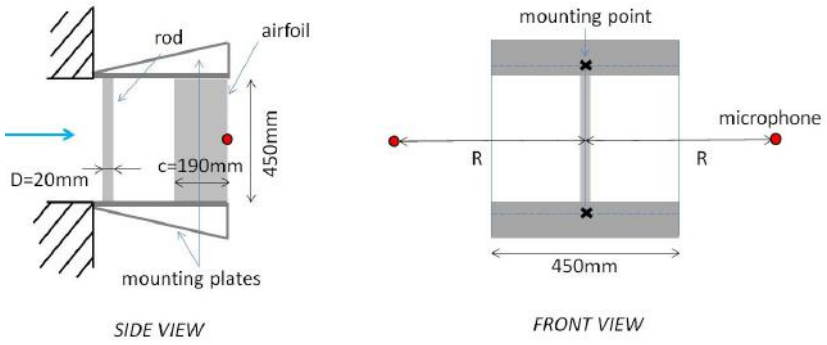

Fig. 2. Sketch-up of rod-airfoil configuration

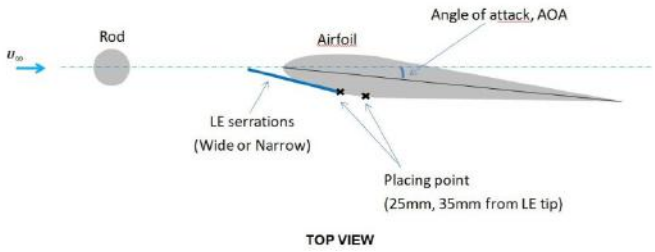

Fig. 3. Schematic diagram of leading edge serrations used and current study

2.2 Hot Wire Anemometer for Velocity Profile Measurement

The hot wire anemometer is used to perform wake survey of the streamwise velocity downstream of the problem configuration (in this study the airfoil wake). Hot wire is a thin cylindrical wire made from tungsten wire with thin platinum coating on its surface. The hot wire compute flow velocity from its relationship between local flow velocity and the convective heat transfer from the heated elements. When air flows over the wire, heat transfer from the wire will act to reduce the wire's temperature and unbalance the bridge. By simultaneously powering the wire and supplying it with current at the same rate at which heat is lost, the bridge can re-balance itself at a rate much faster than the smallest eddies in the flow, and the temperature of the wire can be kept virtually constant in time. The heat loss from the wire (which is directly proportional to the bridge voltage) is then monotonically related to the velocity of the flow.

A miniature wire probe with wire length of 1.2 mm diameter and of 5 μm is used. The hot wire is held by a self-designed traverse (shown in figure) and is connected to the signal analyzer the NI 9233 compact DAQ. Each velocity record is sampled at 2^{15} Hz for 15 seconds. This hot wire is calibrated inside of the AWT. For a calibration, the hot wire is placed on the traverse arm and positioned in the core of the wind tunnel. The wind tunnel is then run at 30 different velocities ranging from zero to 15 m/s. The velocity of the tunnel is monitored using a pitot tube connected to a Baratron transducer via long plastic tubing.

A careful calibration of the constant temperature anemometer is crucial to guarantee high reliable data. In current study, calibration is done to provide relation between velocity and output voltage of the CTA signal. For this purpose, the hot wire is exposed to varying flow speeds at the measurement location while a pitot tube, located to the hot wire measures the dynamic pressure. Use of the ambient temperature and barometric pressure enables the determination of the flow velocity in accordance to the equation below.

$$U_0 = \sqrt{\frac{2 \cdot p_{\mathrm{dyn}}}{\rho}} \tag{1}$$

Relating the output voltage of the anemometer to the measured flow speed yields a calibration curve to be used for further hot wire measurements. The curve fit is performed by use of a polynomial function of 4$^{\mathrm{th}}$ order (Eq. (2)) or the King's Law (Eq. (3)) whereas the polynomic form is expected to yield a higher accuracy. For a calibration in a velocity range of 0 m/s to 20 m/s measurement points where the most points cover the low to intermediate velocity region due to the higher gradient in voltage.

$$E = C_0 + C_1E + C_2E^2 + C_3E^3 + C_4E^4 \quad (2)$$

$$E^2 = C_0 + C_1(U)^n \quad (3)$$

where E is the output voltage, C_0 to C_4 are calculated constants, U the flow velocity and n the scaling power of the velocity.

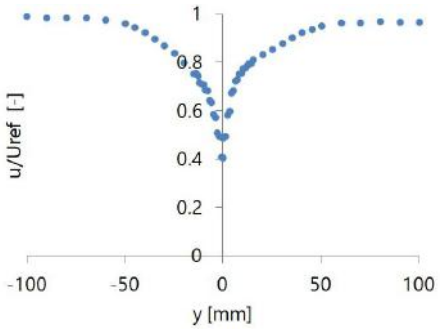

Fig. 4. Velocity profile at x=10mm downstream the airfoil

2.3 Microphone Setup for Sound Measurement

To measure the flow-induced noise, GRAS 40PH microphones are used. The microphones are held using microphone holder as presented in Figure 5. The microphone's frequency range is ±1 dB range between 50-20000 Hz as stated in the transducer documentations. The microphones are located at a distance R=500 mm away from the trailing edge of airfoil at 90 and 180 degree angles to the flow direction directly above and below the airfoil.

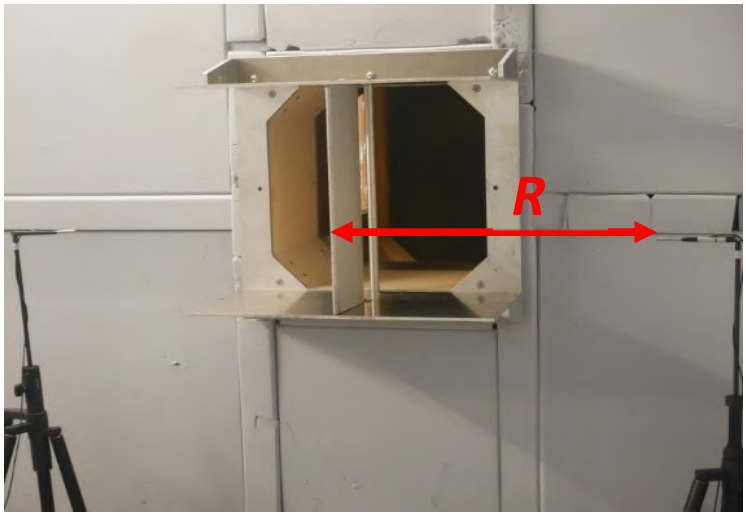

Fig. 5. Microphones position for sound measurement

The acoustic pressure is sampled at 51 200 Hz for 10 seconds using a DAQ with an automatic anti-aliasing filter. Noise measurement from the microphone is obtained in the form of sound pressure fluctuations in Pascal. The sound pressure level in decibels is then calculated using (1).

$$SPL = 20\log\left(\frac{P_I}{P_{\text{ref}}}\right) \text{ [dB]} \quad (4)$$

The reference pressure is $P_{\text{ref}} = 2.0 \times 10^{-5}$ [Pa].

3. Noise Control Setup

Two parameters are being investigated in the effect of sound radiation. They are the serrations wideness (λ) and the location of the serrations (y) are placed are as presented in Fig. 3. The gap between the rod and airfoil is G=3.5D agreeing the study of Y. Li whom proved that at G ≥ 3.3D the airfoil experience fully developed vortex in the wake of the rod (Yong Li *et al.,* [33]). The narrow serrations have constant amplitude of 33.09 mm and wavelength of 8.27 mm, while the wide serrations have the same amplitude but a double wavelength of the narrow serrations'. The serrations are placed at pressure surface of the airfoil. This concept was previously investigated by Hersh *et al.,* [31]. In all cases, the influence of different angles of attack is also investigated.

Table 1
Noise control setup

Type of serrations, λ	Wide	Narrow
Placing point, y	25mm, 35mm from LE	25mm, 35mm from LE
AOA	0°~30°	0°~30°

4. Results

This section summarizes the results of several tests using the aforementioned microphone to identify the serrations effect on the noise generation. The parametric study (including the wideness of serrations and effects of serrations location) is made by comparing the sound spectra in decibels and the integration of sound spectra at different range of sound frequency with the clean rod-airfoil case (without serrations).

4.1 Sound Pressure Fluctuations

Figure 6 shows the time history of sound pressure of the background environment of the tunnel. The background sound is needed prior to observe the changes in the noise level when the rod-airfoil is placed inside the wind tunnel.

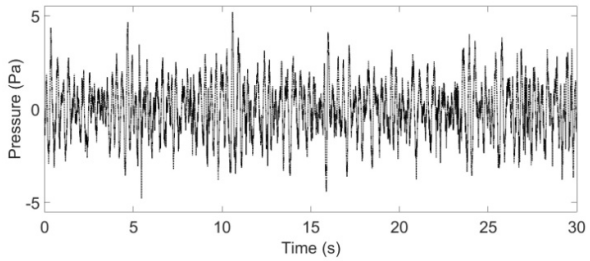

Fig. 6. Sound pressure fluctuations of background noise (without test case)

4.2 Sound Spectra

The sound pressure fluctuation is then transformed using FFT to get the spectra as shown in Figure 7. The figure depicts sound spectrum density of the baseline case. Sound from the rod-airfoil

configuration and the airfoil only cases are compared. The case with upstream rod shows the presence of a tonal peak at a low frequency. The tonal peak is explained due to the vortex shedding of the upstream rod. The interaction between the rod wakes with the leading edge of the airfoil is believed to be the generation mechanism of airfoil-turbulence interaction noise [14]. Current study has taken the integral of the spectra at two different frequency ranges; namely the tonal noise (at frequency in the vicinity of the tonal peak Strouhal number) and the broadband noise (at frequency other than the tonal range). Hence, the tonal noise is calculated to be 1.79 dB and the broadband noise is 2.09 dB. The integral equations for tonal noise and broadband noise are as in Eq. (5) and Eq. (6) respectively. These values will be the baseline case for reference in order to identify the effect of serrations on the noise reduction**.**

$$Tonal\ N\ [dB] = \int_{St=0.1}^{St=0.3} SP\ (St)\ d\ St \tag{5}$$

$$Broadband\ N\ [dB] = \int_{St=0.3}^{St=1.0} SP\ (St)\ d\ St \tag{6}$$

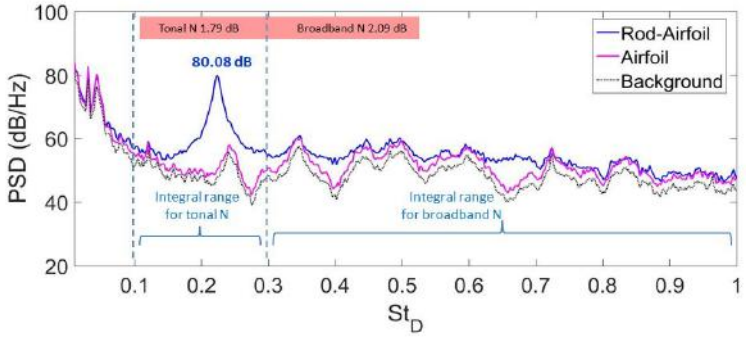

Fig. 7. Sound spectrum density of baseline case (clean rod-airfoil configuration)

Figure 8 represents the sound spectra for cases with the leading edge serrations at two respective angles of attack i.e. AOA=0° and AOA=12°. There is not much obvious reduction if seen from the sound spectra if seen in overall. However, results of the case when angle of attack AOA=12° show that the LE serrations give better noise reduction effect at higher AOA. If seen from the integral values, wide serrations (highlighted in green box) have a bigger noise reduction if compared to that of the narrow serrations. The narrow serrations even increased some noise in the broadband part at zero angle of attack.

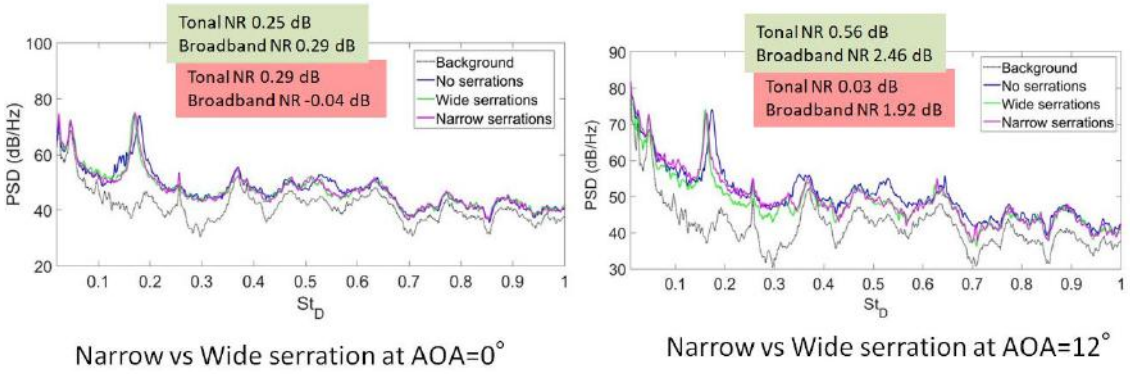

Fig. 8. Sound spectra results for case of wide or narrow LE serrations

4.3 Integration of Sound Spectrum

The relation of the sound reduction ($\Delta\ SPL$) with the angles of attack can be further investigated by referring to the lines in Figure 9. LHS shows the tonal sound and RHS shows the broadband sound. The LE serrations of current study seem to give better noise reduction at angles of attack in the range of approximately 10° to 25°. Highest noise reduction is when the angle of attack is at 12°. Whereas at lower angles of attack cases, the serrations seem to have increased the noise generation.

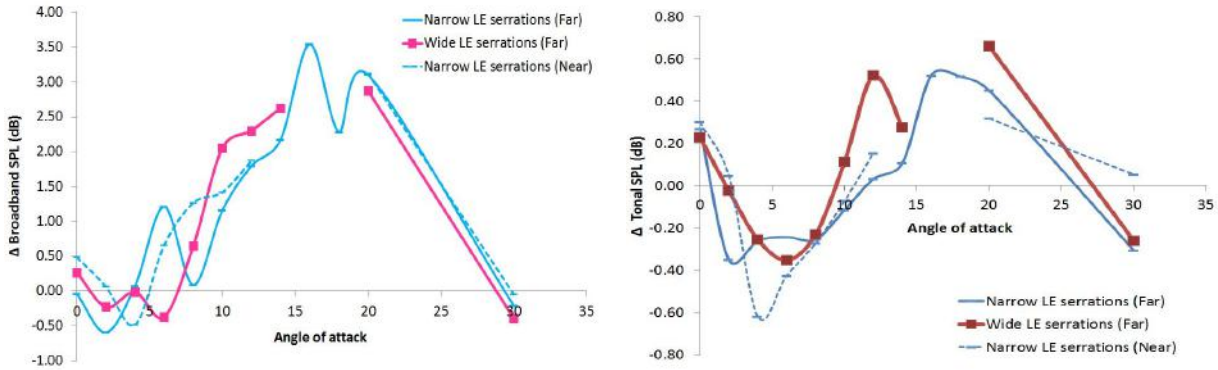

Fig. 9. Tonal (LHS) and broadband (RHS) sound levels at different angles of attack

5. Conclusion

The noise measurement setup of rod-airfoil configuration has been discussed and the LE serrations effect on the noise generation of rod-airfoil has been assessed. Wider serration gives better noise reduction and the LE serrations give good reduction at higher angle of attack. For the future planning, the noise increment and reduction that the LE serrations promote at different angle of attack can be further explained based on the flow behaviours and physics point of view.

Acknowledgement

The author would like to acknowledge University Teknologi Malaysia for the Ainuddin Wahid Scholarship award. Additionally, the research is also sponsored by Malaysia of Higher Education (MOHE) under the Research Grant project of Universiti Teknologi Malaysia (Vot No.R.K130000.7843.4F712). Special thanks to University of New South Wales (UNSW) for the use of wind tunnel facilities and also Assoc Prof Con Doolan for his supervision during the research attachment in UNSW Sydney.

References

[1] Paterson, R., and R. Amiet. "Acoustic radiation and surface pressure characteristics of an airfoil due to incident turbulence." In *3rd Aeroacoustics Conference*, p. 571. 1976.

[2] Migliore, Paul, and Stefan Oerlemans. "Wind tunnel aeroacoustic tests of six airfoils for use on small wind turbines." *Journal of Solar Energy Engineering* 126, no. 4 (2004): 974-985.

[3] Moreau, Stephane, and Michel Roger. "Effect of angle of attack and airfoil shape on turbulence-interaction noise." In *11th AIAA/CEAS aeroacoustics conference*, p. 2973. 2005.

[4] Jackson, R., J. M. R. Graham, and D. J. Maull. "The lift on a wing in a turbulent flow." *The Aeronautical Quarterly* 24, no. 3 (1973): 155-166.

[5] McKeough, P. J., and J. M. R. Graham. "The effect of mean loading on the fluctuating loads induced on aerofoils by a turbulent stream." *The Aeronautical Quarterly* 31, no. 1 (1980): 56-69.

[6] Mish, Patrick Francis. "An experimental investigation of unsteady surface pressure on single and multiple airfoils."

PhD diss., Virginia Tech, 2003.
[7] Haeri, Sina, Jae Wook Kim, Subramanian Narayanan, and Phillip Joseph. "3D calculations of aerofoil-turbulence interaction noise and the effect of wavy leading edges." In *20th AIAA/CEAS Aeroacoustics Conference*, p. 2325. 2014.
[8] Paruchuri, Chaitanya, Narayanan Subramanian, Phillip Joseph, Christina Vanderwel, Jae Wook Kim, and Bharathram Ganapathisubramani. "Broadband noise reduction through leading edge serrations on realistic aerofoils." In *21st AIAA/CEAS Aeroacoustics Conference*, p. 2202. 2015.
[9] Chaitanya, P., Phillip Joseph, Subramanyam Narayanan, Christina Vanderwel, Jacob Turner, Jae-Wook Kim, and Bharathram Ganapathisubramani. "Performance and mechanism of sinusoidal leading edge serrations for the reduction of turbulence–aerofoil interaction noise." *Journal of Fluid Mechanics* 818 (2017): 435-464.
[10] Pope, Stephen B. "PDF methods for turbulent reactive flows." *Progress in energy and combustion science* 11, no. 2 (1985): 119-192.
[11] Gruber, Mathieu, Phillip Joseph, and Mahdi Azarpeyvand. "An experimental investigation of novel trailing edge geometries on airfoil trailing edge noise reduction." In *19th AIAA/CEAS Aeroacoustics Conference*, p. 2011. 2013.
[12] Turner, Jacob, and Jae Wook Kim. "Towards Understanding Aerofoils with Wavy Leading Edges Interacting with Vortical Disturbances." In *22nd AIAA/CEAS Aeroacoustics Conference*, p. 2952. 2016.
[13] Jacob, Marc C., Jérôme Boudet, Damiano Casalino, and Marc Michard. "A rod-airfoil experiment as a benchmark for broadband noise modeling." *Theoretical and Computational Fluid Dynamics* 19, no. 3 (2005): 171-196.
[14] Strouhal, Vincenz. "Über eine besondere Art der Tonerregung." *Annalen der Physik* 241, no. 10 (1878): 216-251.
[15] Zdravkovich, M. M. "Flow around circular cylinders volume 1: fundamentals." *Oxford University Press, Oxford* 19 (1997): 185.
[16] Stapountzis, H., K. Yakinthos, A. Goulas, S. Kallergis, and V. Kambanis. "Cylinder wake: airfoil interaction for application to a downwind HAWT." In *EWEC-CONFERENCE-*, pp. 172-175. 1999.
[17] Cambanis, V. P., and H. Stapountzis. "An experimental study and FLUENT simulation of the horizontal axis wind turbine (HAWT) blade-tower dynamic interaction." In *2nd Southeastern Europe Fluent Users Group Meeting. November*, pp. 1-2.
[18] Takagi, Y., N. Fujisawa, T. Nakano, and A. Nashimoto. "Cylinder wake influence on the tonal noise and aerodynamic characteristics of a NACA0018 airfoil." *Journal of Sound and Vibration* 297, no. 3-5 (2006): 563-577.
[19] Henning, Arne, Kristian Kaepernick, Klaus Ehrenfried, Lars Koop, and Andreas Dillmann. "Investigation of aeroacoustic noise generation by simultaneous particle image velocimetry and microphone measurements." *Experiments in fluids* 45, no. 6 (2008): 1073.
[20] Henning, A., L. Koop, K. Ehrenfried, A. Lauterbach, and S. Kroeber. *Simultaneous multiplane piv and microphone array measurements on a rod-airfoil configuration. 15th AIAA/CEAS Aeroacoustics Conference, Miami*. USA AIAA-2009-3184, 2009.
[21] Lorenzoni, Valerio, Marthijn Tuinstra, Peter Moore, and Fulvio Scarano. "Aeroacoustic analysis of a rod-airfoil flow by means of time-resolved PIV." In *15th AIAA/CEAS Aeroacoustics Conference (30th AIAA Aeroacoustics Conference)*, p. 3298. 2009.
[22] Giesler, Jens, and Ennes Sarradj. "Measurement of broadband noise generation on rod-airfoil-configurations." In *15th AIAA/CEAS Aeroacoustics Conference (30th AIAA Aeroacoustics Conference)*, p. 3308. 2009.
[23] Casalino, Damiano, Marc Jacob, and Michel Roger. "Prediction of rod-airfoil interaction noise using the Ffowcs-Williams-Hawkings analogy." *AIAA journal* 41, no. 2 (2003): 182-191.
[24] Boudet, Jérôme, Nathalie Grosjean, and Marc C. Jacob. "Wake-airfoil interaction as broadband noise source: a large-eddy simulation study." *International Journal of Aeroacoustics* 4, no. 1 (2005): 93-115.
[25] Magagnato, Franco, Esra Sorgüven, and Martin Gabi. "Far Field Noise Prediction by Large Eddy Simulation and Ffowcs Williams Hawkings Analogy." In *9th AIAA/CEAS Aeroacoustics Conference and Exhibit*, p. 3206. 2003.
[26] Greschner, Björn, Frank Thiele, Marc C. Jacob, and Damiano Casalino. "Prediction of sound generated by a rod–airfoil configuration using EASM DES and the generalised Lighthill/FW-H analogy." *Computers & fluids* 37, no. 4 (2008): 402-413.
[27] Berland, Julien, Philippe Lafon, Fabien Crouzet, Frédéric Daude, and Christophe Bailly. "Numerical insight into sound sources of a rod-airfoil flow configuration using direct noise calculation." In *16th AIAA/CEAS Aeroacoustics Conference*, p. 3705. 2010.
[28] Berland, Julien, Philippe Lafon, Fabien Crouzet, Frédéric Daude, and Christophe Bailly. "A parametric study of the noise radiated by the flow around multiple bodies: direct noise computation of the influence of the separating distance in rod-airfoil flow configurations." In *17th AIAA/CEAS Aeroacoustics Conference (32nd AIAA Aeroacoustics Conference)*, p. 2819. 2011.
[29] Haeri, Sina, Jae Wook Kim, Subramanian Narayanan, and Phillip Joseph. "3D calculations of aerofoil-turbulence interaction noise and the effect of wavy leading edges." In *20th AIAA/CEAS Aeroacoustics Conference*, p. 2325.

2014.
[30] Hansen, Kristy L., Richard M. Kelso, and Bassam B. Dally. "Performance variations of leading-edge tubercles for distinct airfoil profiles." *AIAA journal* 49, no. 1 (2011): 185-194.
[31] Hersh, Alan S., Paul T. Sodermant, and Richard E. Hayden. "Investigation of acoustic effects of leading-edge serrations on airfoils." *Journal of Aircraft* 11, no. 4 (1974): 197-202.
[32] Johari, Hamid, Charles W. Henoch, Derrick Custodio, and Alexandra Levshin. "Effects of leading-edge protuberances on airfoil performance." *AIAA journal* 45, no. 11 (2007): 2634-2642.
[33] Li, Yong, Xun-nian Wang, Zheng-wu Chen, and Zheng-chu Li. "Experimental study of vortex–structure interaction noise radiated from rod–airfoil configurations." *Journal of Fluids and Structures* 51 (2014): 313-325.